Proceedings of the 2nd National Aero Propulsion Conference
NAPC-2018
Dec 17-19, 2018, IIT Kharagpur, West Bengal

Paper Number: 95

ACOUSTIC EXCITATION OF SELF-EXCITED ELLIPTIC JET DIFFUSION FLAME

Priy Devvrat Singh
Dept. of Aerospace Engineering
IIST, Thiruvananthapuram.

B. R. Vinoth
Dept. of Aerospace Engineering
IIST, Thiruvananthapuram.

Mahesh S.
Dept. of Aerospace Engineering
IIST, Thiruvananthapuram.

ABSTRACT

The nonlinear response of globally unstable elliptic jet diffusion flame under acoustic excitation is studied experimentally and compared with circular jet diffusion flame. Both circular and elliptical jet diffusion flames were forced near the fundamental frequency of global (self-excited) oscillation and away from the it. When the globally unstable jet flames (circular and elliptic) are excited near the fundamental frequency, both flames get locked into forcing frequency through quasiperiodic state with increase in forcing amplitude. However, if the forcing is away from the natural frequency, the flames gets in to quasiperiodic state but never gets locked with the forcing frequency in the range of forcing amplitude studied in the present work.

INTRODUCTION

The understanding of flame-acoustic interaction is crucial for the control of thermoacoustic instabilities. Researchers have shown that the frequency of non-reacting globally unstable flow can be altered using acoustic excitation near the natural oscillations with high amplitude [Provansal et al. (1981)].

Recent studies show that the acoustic excitation of buoyant diffusion flames in circular nozzle, which is globally unstable, exhibit rich nonlinear behavior when subjected to low and moderate forcing [Juniper et al. 2009, Li and Juniper 2013]. The study of acoustic forcing in simple self-excited flow configurations such as buoyant diffusion flame can help in getting useful insights into the complex thermoacoustic instability issues in practical combustion systems [Juniper et al. 2009, Li and Juniper 2013, Balusamy et al. 2014]. In the present study, the nonlinear response of non-circular (elliptic) jet diffusion flame (Aspect ratio, AR=2) under acoustic excitation investigated and compared with circular jet diffusion flame.

EXPERIMENTAL SETUP DESCRIPTION

The schematic of the experimental setup utilized for the present study is shown in Fig. 1. The nozzles used in this study has AR = 1 (circular nozzle) and 2 (elliptic nozzle) with semi minor axis = 1.5 mm. The nozzle was mounted at the end of a stainless steel settling chamber. The settling chamber has a layer of honeycomb structure and a wire mesh screen for conditioning and establishing uniform flow before it encounters the nozzle. The experiments were performed with 99.5 % pure methane gas and the flow rate was set using Alicat digital mass flow controller. The reference length scale for calculating the Reynolds number ($Re = (\rho V D_{eq})/ \mu$) for the fuel jet emanating from the circular nozzle is the diameter of the circular nozzle whereas the reference length scale for a elliptic nozzle is the equivalent diameter ($D_{eq} = 2(ab)^{1/2}$), where a is the semi major axis, b is the semi minor axis of the elliptical nozzle and V is the fuel velocity at nozzle exit.

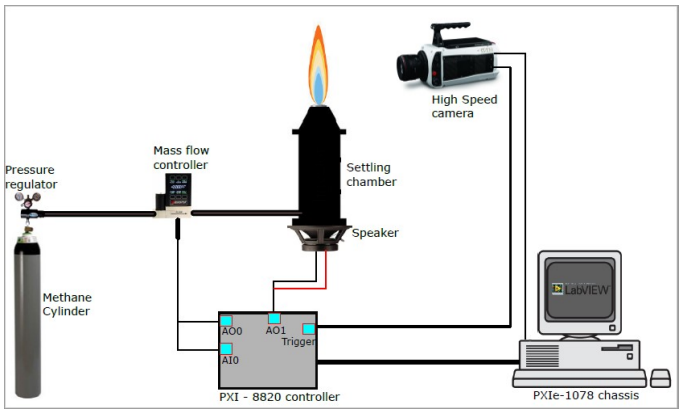

Figure 1. Experimental Setup

Acoustic excitation of the fuel was achieved by fixing a speaker at the bottom of the settling chamber. The speaker used was a 3 inch midrange woofer from AuraSound. The frequency and amplitude input to the speaker was provided by the data acquisition system (DAQ) using LabView program. Natural and forced buoyant jet diffusion flame oscillations were visualized using schlieren (Z-type) optical flow visualization technique. High speed camera (PHANTOM) was used for capturing the schlieren videos at 400 frames per second. The data were recorded simultaneously from both the high-speed camera and the digital mass flow controller using multifunction DAQ device PXIe-6366**.** All the fans, exhausts systems were turned off before commencing the experiment and a relaxation time of 5-10 minutes was provided for ensuring a quiescent ambient within the laboratory.

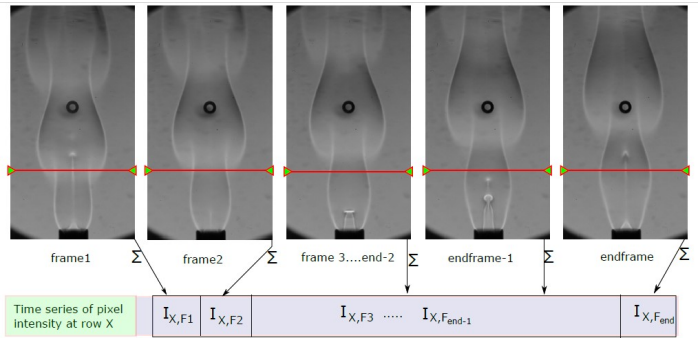

Figure 2. Representation of procedure to obtain time series data from schlieren images at x/D =10.

The schlieren videos of the naturally oscillating and acoustically forced diffusion flame were converted to individual frames. The intensity in each frame is summed across the pixel column at a particular axial location to generate the time series data as shown in Fig. 2. In the present work, the time series data was extracted at x/D = 10, where *D* corresponds to diameter for the circular nozzle whereas it corresponds to the minor axis in the case of elliptic nozzle.

The time series data of the pixel intensity from the schlieren video frames were transformed to Fourier domain using FFT to identify the dominant frequencies in the flame. Nonlinear time series analysis (NTSA) tools such as phase space reconstruction and Poincare map were used to characterize the non-linear behaviour of the flame. The phase space is reconstructed from a scalar times series using Takens time-delay embedding theorem [Takens (1981)]. In order to construct the phase space using the above method, information about the time delay for embedding and embedding dimension are required. In the present study, the optimal time delay for embedding is calculated using average mutual information (AMI) method whereas the minimum embedding dimension is calculated using Cao's method [Cao (1997), Juniper and Sujith (2018)].

RESULTS AND DISCUSSION

Global oscillations

Experiments were performed to understand natural flickering behaviour of elliptic diffusion flame (AR = 2) at different fuel jet Reynolds number. Figure 3 shows the variation of schlieren flow field for elliptic jet diffusion flame when seen from its major side. At low Reynolds numbers, the flame is globally stable, i.e. there is no global oscillation in the flame. At a critical Reynolds number (Re) of 89.64, the flame becomes globally unstable, i.e., the whole flame oscillates at a unique frequency due to buoyancy induced oscillations. The flame shows varicose mode of oscillations as can be seen from the symmetry of vortices structure in Fig. 3. The buoyancy induced vortices size also increases as the Re increases. Similar flow field structures were observed in circular flame as well.

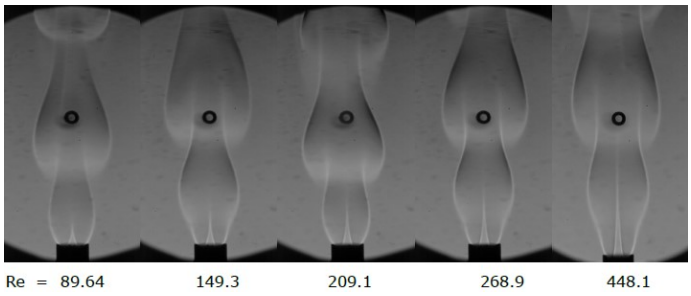

Figure. 3 Variation of schlieren flow field with Reynolds number for elliptic jet diffusion flame (AR = 2).

CIRCULAR JET FLAME EXCITATION

Methane reacting jet (Re = 295.7) from circular nozzle was forced sinusoidally with different amplitude and frequency to study its dynamic response to external forcing. Two forcing cases are reported in this paper viz. (i) $F_f / F_n = 0.95$ and (ii) $F_f / F_n = 0.845$, where F_n is the natural frequency of the jet flame (unforced case) and F_f is the forcing frequency (frequency of acoustic wave). The natural frequency of circular jet flame is 12.42 Hz.

Case 1: Circular jet flame forcing with $F_f/F_n = 0.95$

Circular jet flame was forced at $F_f / F_n = 0.95$ in the amplitude range 25 mV $\leq$ A $\leq$ 125 mV with an increment of 25 mV. Figure 4 shows time series as well as power spectrum of the pixel intensity from the schlieren video frames for all 5 forcing amplitudes. The intensity time series was extracted at x/D = 10. For comparison, the flame without forcing (Amplitude, A=0) is also shown. The spectrum reveal discrete frequencies (fundamental and higher harmonics) which indicate that the flame is self-excited or, in other words, globally unstable.

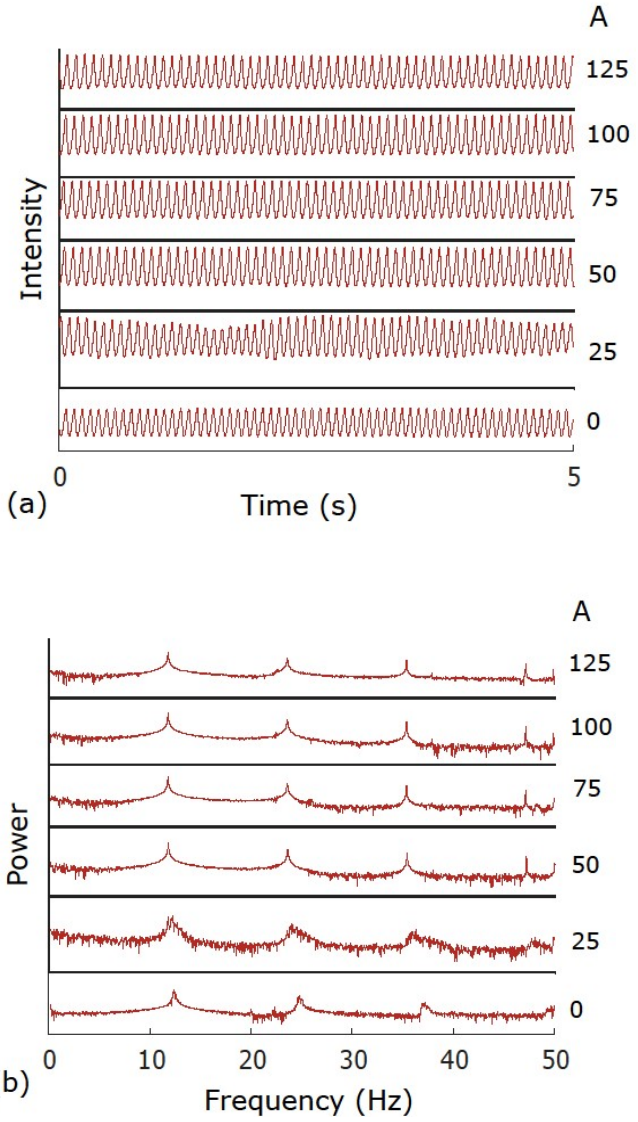

Figure. 4 (a) Time series (b) power spectrum of intensity for circular flame forced at F_f / F_n = 0.95. Data extracted at x/D = 10. The amplitude shown is in mV.

When forced at low amplitude (A = 25 mV), the flame responds at F_n as well as F_f, and the power spectrum shows presence of both natural and forcing frequency, although natural frequency is observed to have higher amplitude. In addition to these two frequencies, there are multiple peaks known as sidebands, which are generated by nonlinear interaction between the natural and forcing mode. As a result, the beating phenomenon can also be seen in the time series signal for A = 25 mV in Fig. 4(a). As the amplitude of acoustic forcing is increased from 25 mV to 50 mV, the power spectrum shows presence of only F_f and its super-harmonics ($2F_f$, $3F_f$, …) with no sign of the existence of natural frequency. This indicates that the flame oscillation is lock-in state with acoustic excitation. Further increase in the amplitude is observed to

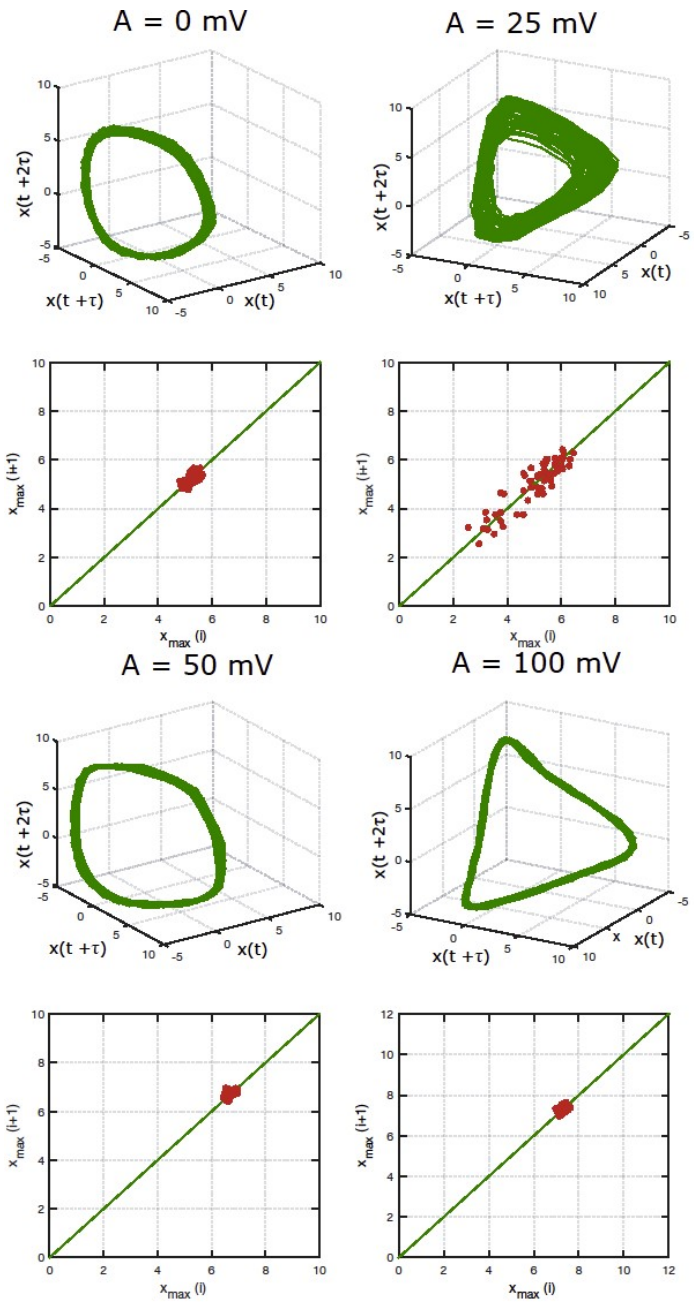

Figure 5. Phase portrait and Poincaré map at different amplitudes for circular flame forced at F_f / F_n = 0.95.

cause no change in the system dynamics.

Figure 5 shows the reconstructed phase space and Poincare map from time series data for A = 0, 25, 50, 100 mV. Note that the Poincare map for each forcing amplitude is shown below the corresponding phase portrait in Fig. 5. For the unforced case, the phase space shows a single closed curve or limit cycle which indicates that there is only one frequency (F_n) in the system. At A = 25 mV, the phase space shows a torus shape indicating presence of two frequencies in the system viz.

natural frequency and forcing frequency. Poincare map for this case shows a set of discrete points in 2D plane approximately forming a ring which indicates that the system is in quasiperiodic state. The excitation at amplitude, A = 50 mV, shows a limit cycle in phase space and a single point in Poincare map which confirms that the natural frequency has locked into forcing frequency and hence $A_{lock\text{-}in}$ = 50 mV for this case. For amplitudes higher than $A_{lock\text{-}in}$ till A = 125 mV, there is no change in the system dynamics and the flame stays locked in. This behavior is consistent with the results of Juniper et al. (2009) and Li and Juniper (2013a).

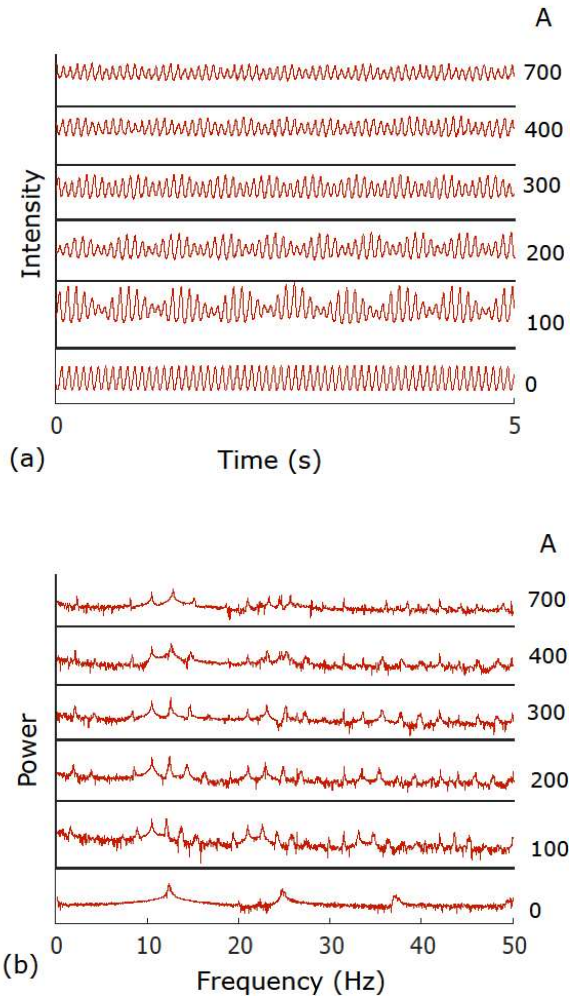

Figure 6. (a) Time series (b) power spectrum of intensity for circular flame forced F_f/F_n = 0.845. Data extracted at x/D = 10. The amplitude shown is in mV.

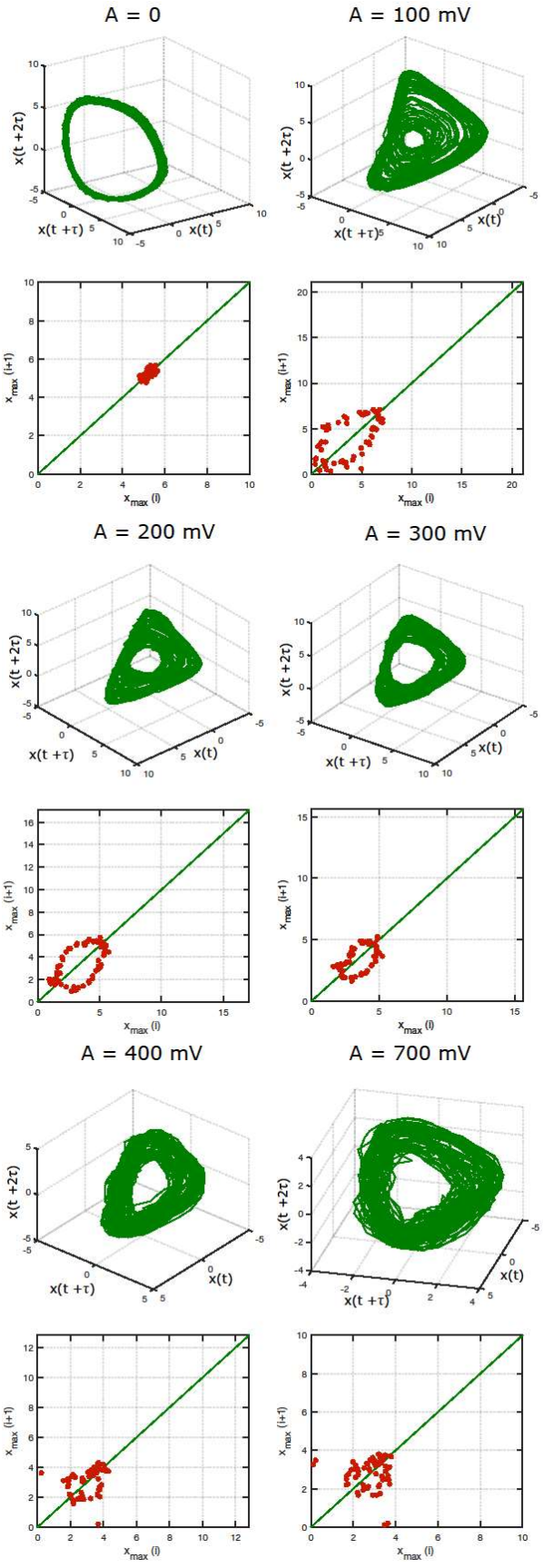

Figure 7. Phase portrait and Poincaré map at different amplitudes for circular flame forced at F_f/F_n = 0.845.

Case 2: Circular jet flame forcing with F_f/F_n = 0.845

The circular jet flame was forced at F_f / F_n = 0.845 which is further away from the natural frequency. The amplitude of forcing is in the range 100 mV ≤ A ≤ 700 mV with increment of 100 mV. Figure 6 shows the time series as well as power spectrum of intensity for all 5 amplitudes. For comparison, flame without forcing case (A=0) is also shown. The power spectrum of forced cases exhibit the spectral peaks around the fundamental as well as forcing frequencies. This is due to non-linear interaction of natural and forcing frequencies. A beat frequency at $|F_f - F_n|$ appears in the power spectrum and the beating can be seen in the corresponding time series signal. Figure 7 shows the phase space and Poincare map for five forcing amplitude and the unforced case. When the forcing amplitude is between 100 mV and 300 mV (100 mV ≤ A ≤ 300 mV), the Poincare map shows a circle which indicates the quasiperiodic state of the system.

If a closer look is taken at the power spectrum, it can be noted that the natural frequency in the forced flame is less than the natural frequency of the unforced flame. The above behavior is called 'frequency pulling' i.e., the natural frequency

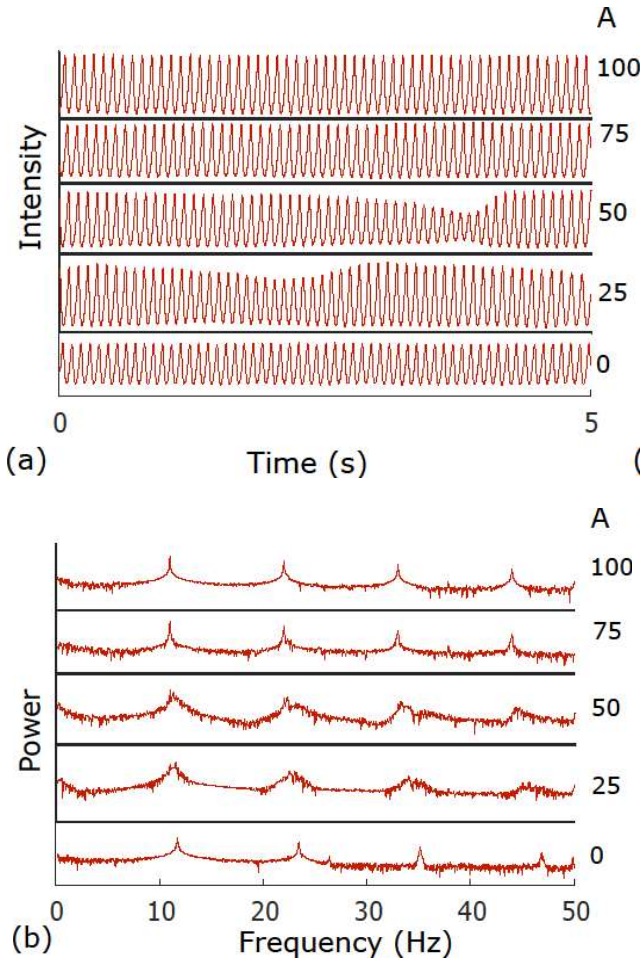

Figure 8. (a) Time series (b) power spectrum of intensity for elliptic flame (AR = 2) forced at F_f/F_n = 0.937. Amplitude shown is in mV.

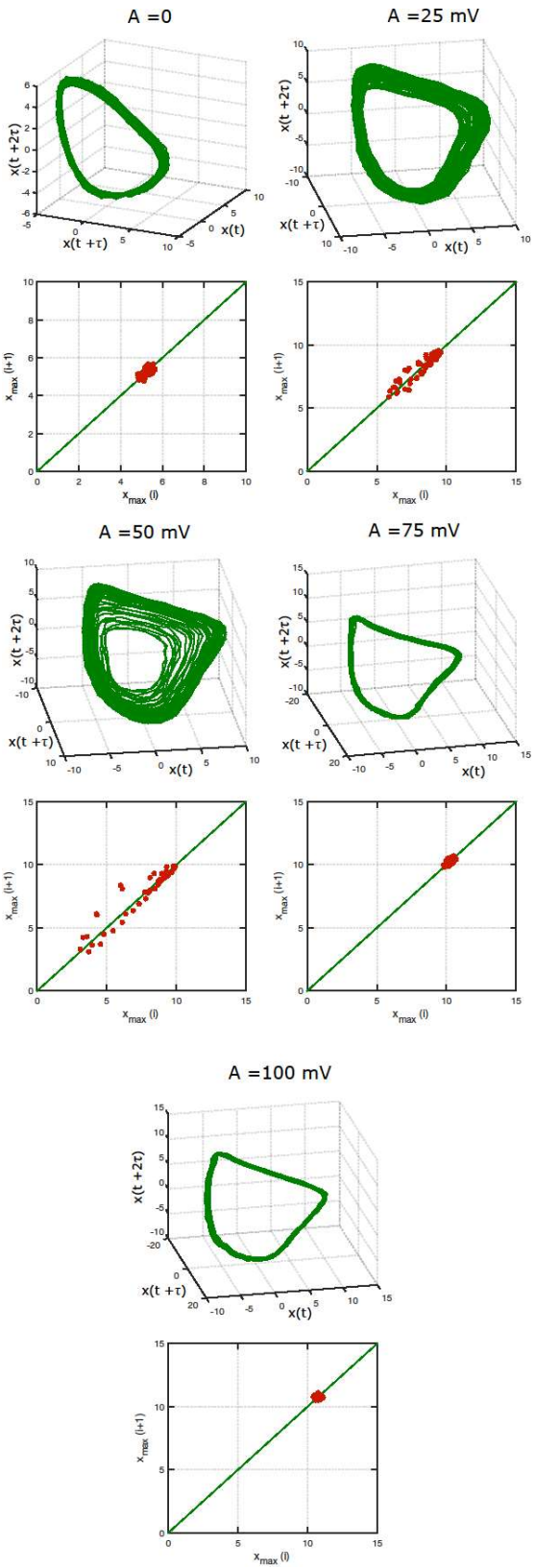

Figure 9. Phase portrait and Poincare map at different amplitudes for elliptic flame (AR = 2) forced at F_f/F_n = 0.937.

of the forced case shift towards the forcing frequency [Li and Juniper (2013b)]. Further increase in the amplitude (till A=700 mV), the spectrum shows the presence of many discrete frequencies which indicate that the flame is not locked into forcing frequency.

ELLIPTIC JET FLAME EXCITATION

Elliptic jet flame (AR=2, Re = 239) was forced sinusoidally with different amplitude and frequency to study its dynamic response to external excitations. Two forcing cases were reported in this paper viz. (i) F_f / F_n = 0.937 and (ii) F_f / F_n = 0.844. The unforced elliptic jet flame shows natural global oscillations at 11.73 Hz.

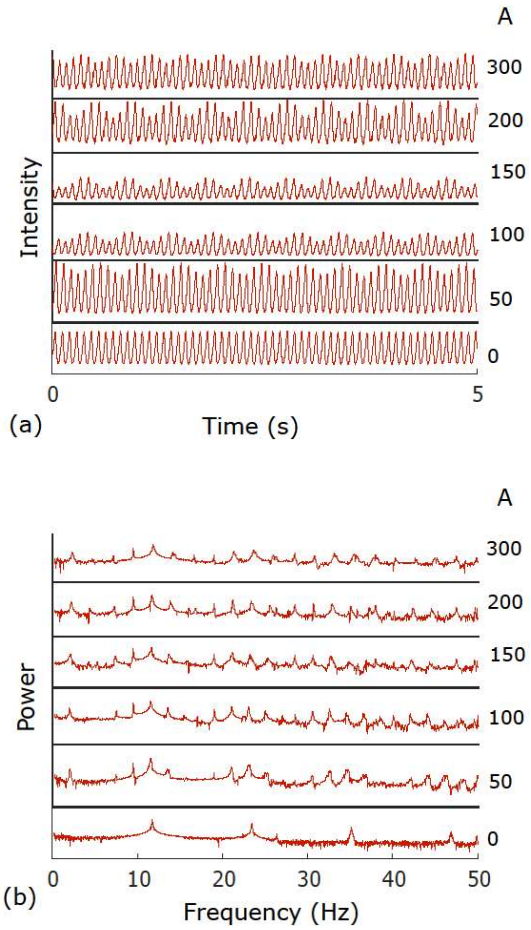

Figure 10. (a) Time series (b) power spectrum of intensity for elliptic flame (AR = 2) forced at F_f/F_n = 0.844. Amplitude shown is in mV.

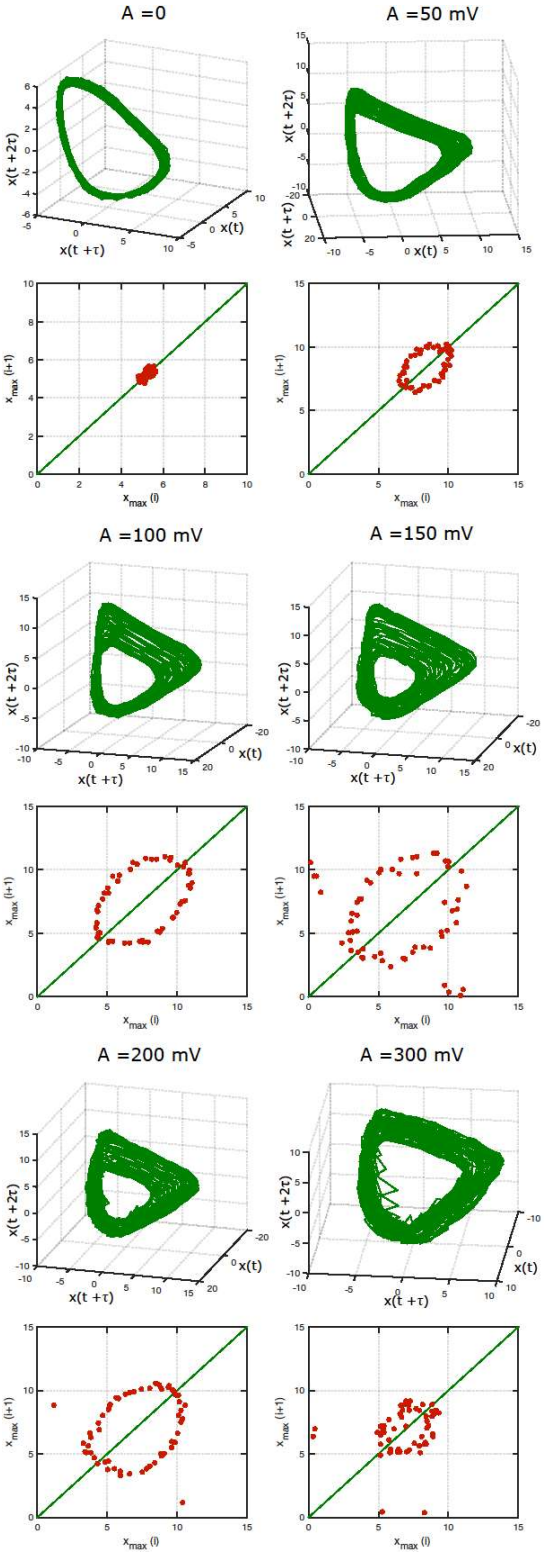

Figure 11. Phase portrait and Poincare map at different amplitudes for elliptic flame (AR = 2) forced at F_f/F_n = 0.844.

Case 1: Elliptic jet flame forcing with $F_f/F_n = 0.937$

The elliptic flame of AR=2 was forced at $F_f/F_n = 0.937$ at varying amplitudes. When forced at A = 50 mV, the power spectrum in Fig. 8 shows the interaction between forcing and fundamental frequency which leads to spectral peaks and beating in time series signal. The phase portrait for A = 50 mV in Fig. 9, shows toroidal structure and Poincare map shows an approximate ring which indicate the system is in quasiperiodic state. Furthermore, increasing the amplitude causes the flame to get lock into forcing frequency at $A_{lock\text{-}in}$ = 75 mV and the power spectrum shows no sign of natural frequency. In summary, the flame went from limit cycle at natural frequency to lock-in at forced frequency through quasiperiodic state. The response of the elliptic flame (AR=2) due to forcing is similar to the forcing response of circular flame.

Case 2: Elliptic jet flame forcing with $F_f/F_n = 0.844$

Figure 10 shows the time series and power spectrum of elliptic flame (AR=2) when forced away from natural frequency at F_f/F_n = 0.844. Power spectrum shows that the system competes between natural and forcing frequency leading to beat frequency for the amplitude range studied. The torus shape in phase portrait and a closed figure in Poincare map shown in Fig. 11, indicates that the system is in quasiperiodic state. The size of the ring in the Poincare map increases with increase in forcing amplitude up to A = 150 mV, then decreases with further increase in amplitude. The flame didn't get lock in to forcing frequency in the range of amplitude studied. This behavior is qualitatively similar to circular jet flame.

CONCLUSIONS

The experimental studies were carried out to investigate the acoustic forcing response of globally unstable elliptic jet diffusion flame and compare its dynamics with globally unstable circular jet diffusion flame. The acoustic forcing was applied near the natural frequency of the oscillating flames and away from the natural frequency at varying amplitudes. The results indicate that when forced very close to natural frequency ($F_f/F_n \approx 0.95$), the response for both elliptic and circular diffusion flames is to reach lock-in state through quasiperiodic state. However, the lock-in amplitude is different for both flames owing to the varying strengths of global instability in the flames. When forced away from the natural frequency ($F_f/F_n \approx 0.84$), both flames remain in quasiperiodic state and didn't lock into the forcing frequency for the range of amplitude studied. The present study shows that the response of circular and elliptic (AR=2) flame behaviors are qualitatively same when forcing frequency is near to the fundamental and slightly away from the fundamental frequency.

REFERENCES

1. Balusamy, S. and Li, L. K. B. and Han, Z. and Juniper, M. P. and Hochgreb S. (2014). Nonlinear dynamics of a self-excited thermoacoustic system subjected to acoustic forcing, *Proceedings of the Combustion Institute*, Vol. 35, 426-437.

2. Cao, L. (1997), 'Practical method for determining the minimum embedding dimension of a scalar time series', Physica D: Nonlinear Phenomena 110(1-2), 43–50.

3. Juniper, M. P. and Sujith, R. I. (2018). Sensitivity and nonlinearity in Thermoacoustics, *Annual Review of Fluid Mechanics,* Vol. 50, 661-689.

4. Li, L. K. B. and Juniper, M. P. (2009). Forcing of self-excited round jet diffusion flames. *Proceedings of the Combustion Institute*, Vol. 32, 1191-1198.

5. Li, L. K. B. and Juniper, M. P. (2013a). Lock-in and quasiperiodicity in hydrodynamically self-excited flames: experiments and modelling. *Proceedings of the Combustion Institute*, Vol. 34, 947-954.

6. Li, L. K. B. and Juniper, M. P. (2013b). Lock-in and quasiperiodicity in a forced hydrodynamically self-excited jet, *Journal of Fluid Mechanics*, Vol. 726, 624-655.

7. Provansal, M., Mathis, C., and Boyer, L. (1987). Benard-von Karman Instability: transient and forced regimes. *Journal of Fluid Mechanics*, Vol. 182, 1-22.

8. Takens, F. (1981), Detecting strange attractors in turbulence, in 'Dynamical systems and turbulence, Springer, pp. 366–381.